



Providing Choice & Value

Generic CT and MRI Contrast Agents

**FRESENIUS
KABI**

CONTACT REP

AJNR

This information is current as
of July 29, 2025.

**[¹⁸F]-FDG Uptake as a Marker of Residual
Anaplastic and Poorly Differentiated Thyroid
Carcinoma following *BRAF*-Targeted
Therapy**







Samir A. Dagher, Kim O. Learned, Richard Dagher, Jennifer
Rui Wang, Xiao Zhao, S. Mohsen Hosseini, Anastasios
Maniakas, Maria E. Cabanillas, Naifa L. Busaidy, Ramona
Dadu, Priyanka Iyer, Mark E. Zafereo and Alexander M.
Khalaf

AJNR Am J Neuroradiol 2025, 46 (6) 1260-1267

doi: <https://doi.org/10.3174/ajnr.A8588>

<http://www.ajnr.org/content/46/6/1260>

[¹⁸F]-FDG Uptake as a Marker of Residual Anaplastic and Poorly Differentiated Thyroid Carcinoma following *BRAF*-Targeted Therapy

 Samir A. Dagher,  Kim O. Learned,  Richard Dagher, Jennifer Rui Wang, Xiao Zhao, S. Mohsen Hosseini, Anastasios Maniakas,  Maria E. Cabanillas, Naifa L. Busaidy, Ramona Dadu, Priyanka Iyer,  Mark E. Zafereo, and  Alexander M. Khalaf



ABSTRACT

BACKGROUND AND PURPOSE: Neoadjuvant *BRAF*-directed therapy and immunotherapy followed by surgery improves survival in patients with *BRAF*^{V600E}-mutant anaplastic thyroid carcinoma (ATC), more so in those who have complete ATC pathologic response. This study assesses the ability of FDG-PET to noninvasively detect residual high-risk pathologies including ATC and poorly differentiated thyroid carcinoma (PDTC) in the preoperative setting.

MATERIALS AND METHODS: This retrospective, single-center study included consecutive *BRAF*^{V600E}-mutant patients with ATC treated with at least 30 days of neoadjuvant *BRAF*-directed therapy and who underwent FDG-PET/CT within 30 days before surgery. The highest pathologic grade observed for every head and neck lesion resected was recorded. Each lesion on preoperative PET/CT was retrospectively characterized. The primary end point was to contrast the standardized uptake normalized by lean body mass (SULmax) for lesions with residual high-risk (ATC, PDTC) versus low-risk pathologies (papillary thyroid carcinoma, negative). An optimal SULmax threshold was then identified by using a receiver operating characteristic analysis, and the ability of this threshold to noninvasively and preoperatively risk-stratify patients by overall survival was then evaluated with a Kaplan-Meier plot.

RESULTS: Thirty patients (mean age 66.5 ± 9.0; 17 men) were included in this study, with 94 surgically sampled lesions. Of these lesions, 57 (60.6%) were low-risk (39 negative, 18 papillary thyroid carcinoma) and 37 (39.4%) were high-risk (29 ATC, 8 PDTC). FDG uptake was higher for high-risk compared with low-risk pathologies: median SULmax 5.01 (interquartile range [IQR] 2.81–10.95) versus 1.29 (IQR 1.06–3.1) (*P* < .001, Mann-Whitney *U* test). The sensitivity, specificity, and accuracy for detecting high-risk pathologies at the optimal threshold of SULmax ≥ 2.75 were 0.784 [95% CI, 0.628–0.886], 0.702 [95% CI, 0.573–0.805], and 0.734 [95% CI, 0.637–0.813], respectively. Patients with at least 1 high-risk lesion identified with the aforementioned cutoff had a worse prognosis compared with patients without high-risk lesions in the head and neck: median overall survival for the former group was 259 days and was not attained for the latter (*P* = .038, log-rank test).

CONCLUSIONS: Preoperative FDG-PET noninvasively identifies lesions with residual high-risk pathologies following neoadjuvant *BRAF*-directed targeted therapy and immunotherapy for *BRAF*-mutated ATC. FDG-PET avidity may serve as an early prognostic marker that correlates with residual high-risk pathology in *BRAF*-mutated ATC after neoadjuvant therapy.

ABBREVIATIONS: ATC = anaplastic thyroid carcinoma; IQR = interquartile range; OS = overall survival; PDTC = poorly differentiated thyroid carcinoma; PTC = papillary thyroid carcinoma; ROC = receiver operating characteristic; SUL = standardized uptake value normalized by lean body mass

Anaplastic thyroid carcinoma (ATC) is rare among thyroid-derived tumors, representing only 1.7% of all thyroid cancer diagnoses in the United States.¹ Despite this rarity, it is responsible for approximately one-half of all thyroid cancer-associated

deaths. All ATCs are categorized as stage IV at the time of diagnosis regardless of disease extent, because of their aggressive and rapidly progressive clinical behavior. ATC arises from thyroid follicular cells and is thought to occur either in isolation or from malignant transformation of more differentiated thyroid carcinomas. The latter is supported by previous research showing that most ATCs arise concurrently or in patients with histories of differentiated thyroid carcinomas, most commonly papillary thyroid carcinoma (PTC), followed by poorly differentiated thyroid carcinoma (PDTC).² PDTC is considered an intermediate grade between the well-differentiated thyroid carcinomas (eg, PTC) and ATC, which itself has a broader spectrum of patient

Received August 25, 2024; accepted after revision November 10.

From the Departments of Neuroradiology/Head and Neck Imaging (S.A.M., K.O.L., R.D., A.M.K.), Head and Neck Surgery (J.R.W., X.Z., A.M., M.E.Z.), Pathology (S.M.H.), and Endocrine Neoplasia and Hormonal Disorders (M.E.C., N.L.B., R.D., P.I.), The University of Texas MD Anderson Cancer Center, Houston, Texas.

Please address correspondence to Alexander M. Khalaf, MD, 1400 Pressler St, Houston, TX, 77030; e-mail: AKhalaf@mdanderson.org



Indicates article with supplemental data.

<http://dx.doi.org/10.3174/ajnr.A8588>

SUMMARY

PREVIOUS LITERATURE: *BRAF*^{V600E}-mutant ATCs are now treated with *BRAF*/MEK-directed therapy before consolidative surgery. This new paradigm has contributed to the improved survival of this patient subpopulation. ATCs are known for their aggressiveness, and high FDG avidity. In some patients, anaplastic foci may coexist with different pathologies such as PDTC and PTC. However, the role of FDG-PET/CT in assessing sites of residual disease, discriminating different histopathologies, and predicting patient outcomes after neoadjuvant targeted therapy remains poorly understood.

KEY FINDINGS: High-risk lesions (ATC, PDTC) exhibit significantly higher FDG uptake than low-risk lesions (PTC, negative), with an optimal standardized uptake normalized by lean body mass threshold of 2.75 achieving a sensitivity = 0.784 [95% CI, 0.628–0.886] and specificity = 0.702 [95% CI, 0.573–0.805]. Patients harboring a single high-risk lesion on preoperative FDG-PET/CT have a worse prognosis with a median overall survival = 259 days.

KNOWLEDGE ADVANCEMENT: In patients with *BRAF*^{V600E}-mutant ATC who underwent neoadjuvant *BRAF*-targeted therapy, FDG uptake reasonably identifies sites of residual high-risk pathologies that negatively impact patient outcomes. Preoperative FDG-PET/CT could thus assist in surgical planning and predicting.

outcomes, but which does include aggressive disease courses, as is suggested by the 22.3% rate of distant metastases and a median survival of 3.8 years.³

The treatment of ATC has dramatically changed over the past decade, with the introduction of *BRAF*/MEK inhibitor therapy, which is effective in the approximately 40% of patients with ATC with tumor expression of a *BRAF*^{V600E} mutation.⁴ In 2018, the FDA approved the *BRAF* inhibitor, dabrafenib, in combination with the MEK inhibitor, trametinib, for the treatment of locally advanced or metastatic *BRAF*^{V600E}-mutant ATC.⁵ Per the American Thyroid Association guidelines and the 2024 Facilitating Anaplastic Thyroid Cancer Specialized Treatment Multidisciplinary Group Consensus Statement, those patients demonstrating favorable treatment response to this regimen can then be considered for consolidative local therapy to control residual sites of macroscopic disease.⁶ This new paradigm has in part contributed to the markedly improved survival of patients with ATC, with prior research from our institution reporting a 35% 1-year survival in patients presenting from 2000–2013, increasing to 59% for those presenting from 2017–2019.⁷ A more recent study demonstrated a 93.6% 1-year survival in patients treated with *BRAF*/MEK inhibitors before surgery, compared with 74.1% in those treated with surgery alone, and 38.5% in those without surgery.⁸ Most patients in this study had also received pembrolizumab, an immune checkpoint inhibitor that significantly prolonged survival according to another recent study by the same group.⁹

After a neoadjuvant course of dabrafenib and trametinib with or without immunotherapy, consolidative therapy most commonly takes the form of surgical resection. The goal of surgery is to resect all neoplastic disease irrespective of histopathology, and for which diagnostic imaging can be valuable in identifying residual tumor. Pretreatment full body imaging with FDG-PET/CT, and/or diagnostic CT or MRI is currently recommended to establish an imaging baseline,^{6,10,11} but no formal guidelines or standard of care have been established regarding the use of imaging both during and following this neoadjuvant course. Because ATC is known to be the most reliably FDG-avid thyroid cancer type

because of its aggressive high-grade histology, FDG-PET/CT has emerged as a potential arbiter for sites of residual tumor in patients treated with *BRAF*-directed therapies.¹² In conjunction with anatomic imaging, sites of qualitatively elevated FDG uptake currently help surgeons decide on their planned approach and scope of resections with the assumption that these sites represent residual tumor. However, limited research has been undertaken to formally assess the reliability of FDG-PET in diagnosing the histologic presence of residual ATC, and no research to our knowledge has addressed this in the context of neoadjuvant *BRAF*-directed therapy and immunotherapy. Therefore, the purpose of this study was to quantitatively evaluate the ability of FDG-PET to correctly diagnose sites of residual ATC and PDTC after *BRAF*-directed therapy and immunotherapy, and secondarily to assess how postneoadjuvant FDG uptake may be associated with patient survival.

MATERIALS AND METHODS

Patient Selection

This is a single-center, Health Insurance Portability and Accountability Act-compliant, institutional review board-approved retrospective cohort study with a waiver of informed consent. The study included consecutively sampled adult patients 1) with biopsy-proved *BRAF*^{V600E}-mutant ATC, 2) who underwent surgical resection between January 2017 and July 2023 after at least 30 days of neoadjuvant combined *BRAF*/MEK-directed therapy with or without immunotherapy, and 3) who underwent FDG-PET/CT within 30 days before surgery. The latter was intended to ensure the pathologic diagnosis at the time of the scan closely resembles the pathologic state at the time of surgery. *BRAF*-directed therapy consisted of dabrafenib, vemurafenib, encorafenib, or sorafenib while MEK-directed therapy included trametinib, cobimetinib, binimetinib, or selumetinib. Immunotherapy consisted of monoclonal antibodies targeting PD-1 or PD-L1 checkpoint proteins such as pembrolizumab or atezolizumab. The ensuing article adheres to the Standards for Reporting of Diagnostic Accuracy Studies checklist for diagnostic accuracy studies (Supplemental Data).¹³

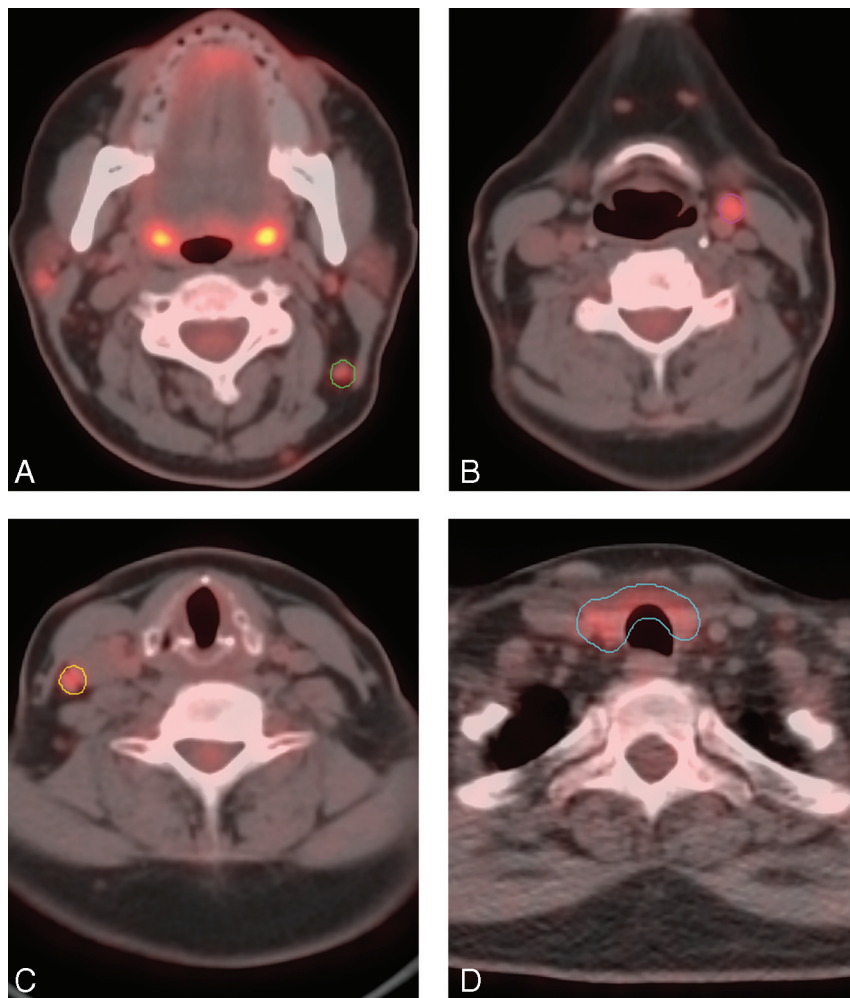


FIG 1. Correlation between pathology report and preoperative FDG-PET/CT in a 53-year-old female patient with ATC stage IVB, status post 3.5 months of neoadjuvant dabrafenib/trametinib. *A*, Lymph node cluster contoured in *green*, labeled as “Neck, left level IIb, dissection: 4 lymph nodes, negative for tumor (0/4)” on the pathology report. *B*, Lymph node cluster contoured in *purple*, labeled as “Neck, left level III, dissection: metastatic anaplastic thyroid carcinoma in 1 of 12 lymph nodes (1/12); tumor size of 1.5 cm with no extranodal extension” on the pathology report. *C*, Lymph node cluster contoured in *yellow*, labeled as “Neck, right level III, dissection: 4 lymph nodes, negative for tumor (0/4)” on the pathology report. *D*, Thyroid tissue contoured in *bright blue*, labeled as “Thyroid, total thyroidectomy: extensive treatment effect with complete response; exuberant lymphocytic thyroiditis and follicular atrophy with few remaining thyroid follicles” on the pathology report.

Molecular Imaging Protocol

Participants were required to fast for at least 4 hours before radiotracer injection. Baseline blood glucose levels were measured to confirm values remained below 200 mg/dL. Injected doses of FDG-PET/CT ranged from 7–12 mCi and were administered intravenously through an 18- to 24-gauge intravenous catheter followed by a 20 mL saline flush. Pre- and postadministration of the radiotracer, patients were isolated in a quiet, dim environment and advised to minimize speaking, movement, and exposure to other stimulatory activities. The interval between the administration of the radiotracer and the onset of image acquisition was approximately 60 minutes. PET scans were conducted with the patient in a single bed position, focusing on the neck as well as the whole body (from skull base to mid thighs) utilizing

3D and TOF techniques, with contemporaneous low-dose noncontrast CT performed for attenuation correction. Additional parameters included a 10-minute static image acquisition phase, a matrix of 256×256 , and a diagonal FOV of 30 cm.

Clinical, Pathologic, and Imaging Data

Demographic and clinical characteristics were retrospectively extracted from electronic medical records, including age, sex, neoadjuvant treatment course, and survival data. Postoperative pathology reports were also extracted from patient charts. Of note, pathologic assessment was performed on standard hematoxylin and eosin–stained surgical specimens by board-certified pathologists. The detailed anatomic location of each resected lesion was recorded from the pathology reports as follows. For the resected primary thyroid mass, the laterality, as well as the anatomic structure(s) abutted or invaded in the pathologic sample (eg, internal carotid, sternocleidomastoid, strap muscles, tracheal wall, laryngeal cartilages, esophagus, or manubrium) were recorded. For each lesion sampled from lymph node groups, the total number of lymph nodes examined, the number of lymph nodes positive for tumor, the laterality of the lymph node group, and the group level as per Robbins et al¹⁴ were recorded. The latter classification scheme has been adopted by all neuro-radiologists, head and neck surgeons, and pathologists at our institution. In some cases, the primary thyroid mass was confluent with adjacent metastatic adenopathy, and thus these were

grouped together as a single lesion on the pathology report and in our analysis. The highest pathologic grade corresponding to each of these lesions was noted as a multilevel categorical variable: no tumor, PTC, PDTC, or ATC.

Each lesion as defined above was then retrospectively correlated to the preoperative FDG-PET/CT by a dual-board-certified neuroradiologist and nuclear medicine physician with the aid of a research associate. To increase the confidence of correctly correlating lesions from the surgical pathology reports to those on the preoperative FDG-PET/CT, operative reports for each case as well as contemporaneous anatomic imaging (ie, diagnostic CT and MRI) were consulted. This correlation is illustrated in Fig 1. Each lesion was subsequently segmented by using the PETEdge+ tool of MIM Software Version 7.2 (MIM Software), and its

Table 1: Baseline characteristics for *BRAF*^{V600E}-mutant patients with ATC (n=30)

Baseline Characteristic	Summary Statistic
Age at surgery, mean (standard deviation)	66.5 (9.0)
Sex, frequency (percent)	
Men	17 (56.7%)
Women	13 (43.3%)
AJCC Eighth Edition stage, ³⁰ frequency (percent)	
IVB	15 (50.0%)
IVC	15 (50.0%)
Days of neoadjuvant BRAF/MEK inhibitor therapy, median (IQR)	103.5 (79.8–196.5)
Immunotherapy before and/or after surgery, frequency (percent)	28 (93.3%)
Pembrolizumab	25 (89.3%)
Atezolizumab	3 (10.7%)
Surgically sampled lesions with known pathology	
Low risk (no tumor, PTC)	57 (60.6%)
High risk (PDTC, ATC)	37 (39.4%)

Note:—AJCC indicates American Joint Committee on Cancer Classification.

maximum standardized uptake value normalized by lean body mass (SULmax) was recorded. Normalization by lean body mass was used to enhance the accuracy and comparability of FDG uptake measurements in our cohort of patients with heterogeneous body compositions.^{15,16} In accordance with the PET Response Criteria in Solid Tumors guidelines developed by Wahl et al,¹⁷ the liver SULmean uptake was used as an internal reference to compare against anatomic imaging sites/surgical pathology samples. If these sites had uptake above liver SULmean, their uptake parameters were collected for analysis, but if their uptake was below liver SULmean, they were imputed with the SULmean of the carotid artery so as to most accurately reflect background metabolic activity in the neck.

Statistical Analysis

Qualitative and quantitative variables were summarized with their frequency (percent) and median (interquartile range [IQR]), respectively. The primary end point of this study was to contrast SULmax for lesions with residual high-risk (ATC, PDTC) versus low-risk pathologies (PTC, negative) by using the Mann-Whitney *U* test. These pathologies were grouped as such due to their overlap in clinical outcomes and previous research demonstrating comparable FDG avidity.^{12,18,19} As part of an exploratory analysis, the Kruskal-Wallis test followed by Dunn test with Bonferroni adjustment were conducted to compare the distributions of SULmax across all 4 pathologic assessments. The discriminative ability of SULmax was then evaluated with a receiver operating characteristic (ROC) analysis and the area under the curve was computed. Confusion matrices were generated at various SULmax thresholds, including the optimal threshold with the highest Youden index (sensitivity + specificity – 1) and the sensitivity, specificity, and accuracy were derived for each of these cutoffs.^{20,21} These results were examined in conjunction with a board-certified head and neck surgeon to identify a clinically meaningful SULmax threshold maximizing the sensitivity of detection of residual, high-risk pathologies before consolidative surgery. Finally, a Kaplan-Meier analysis was utilized to explore the association between preoperative SULmax and overall survival (OS). OS was defined as the time interval between surgery and death with right-censoring at last documented follow-up.

Data analysis was conducted on SPSS Version 29.0 (IBM), and level of significance was set at .05.

RESULTS

Patient Characteristics

Of 55 potentially eligible *BRAF*^{V600E}-mutant ATC patients being treated at our institution between January 2017 and July 2023 who received preoperative FDG-PET/CT, 25 were excluded due to their preoperative PET examination being more than 30 days before their surgical resection date, resulting in 30 patients being included in this study. The mean age was 66.5 ± 9.0 years (range 46.7–79.7), and 17 patients (56.7%) were men. Fifteen patients (50.0%) had stage IVB disease while 50.0% had stage IVC disease. Twenty-eight of 30 (93.3%) patients received immunotherapy before and/or after surgery with pembrolizumab (25/28, 89.3%) or atezolizumab (3/28, 10.7%). The median duration of neoadjuvant BRAF/MEK inhibitor treatment was 103.5 days (IQR 79.8–196.5). The median time from preoperative FDG-PET/CT acquisition and surgery was 7.0 days (IQR 3.5–18.3). Among the 94 surgically sampled lesions, 29 (30.9%) had residual ATC, 8 lesions (8.5%) had PDTC, 18 (19.1%) had PTC, and 39 (41.5%) did not have histopathologic evidence of residual thyroid carcinoma. The baseline characteristics of our cohort are summarized in Table 1.

FDG Uptake and Thyroid Cancer Subtype

Among the 94 surgically sampled lesions, 37 (39.4%) harbored a high-risk histopathologic subtype while 57 (60.6%) did not and were considered low-risk lesions. There was no significant association between the duration of targeted therapy and preoperative FDG-uptake for all lesions (Kendall τ -b = 0.089, *P* = .228). The median SULmax for high-risk lesions was 5.01 [IQR 2.81–10.95]. This was significantly different from the median SULmax for low-risk lesions equal to 1.29 [IQR 1.06–3.1] (*P* < .001, Mann-Whitney *U* test). The distributions of SULmax values for each risk group are illustrated in Fig 2. Additionally, there was a significant difference between the median SULmax for all cancer types grouped together, which was 4.32 [IQR 1.94–10.84], and the median SULmax at sites of no residual tumor, which was 1.22 [IQR 1.04–2.54] (*P* < .001, Mann-Whitney *U* test). Although the distribution of SULmax values differed across all 4 histopathologic diagnoses (*P* < .001, Kruskal-Wallis test), post hoc comparisons only revealed a significant difference in median SULmax values between lesions containing residual ATC and those without residual tumor (adjusted *P* < .001). The distributions of SULmax values for each histopathologic diagnosis are shown in Fig 3 and representative cases are displayed in Fig 4.

Threshold Analysis

The ROC curve in Fig 5, which illustrates the trade-off between sensitivity and specificity across a range of SULmax thresholds, revealed an area under the curve of 0.793 [95% CI, 0.702–0.884].

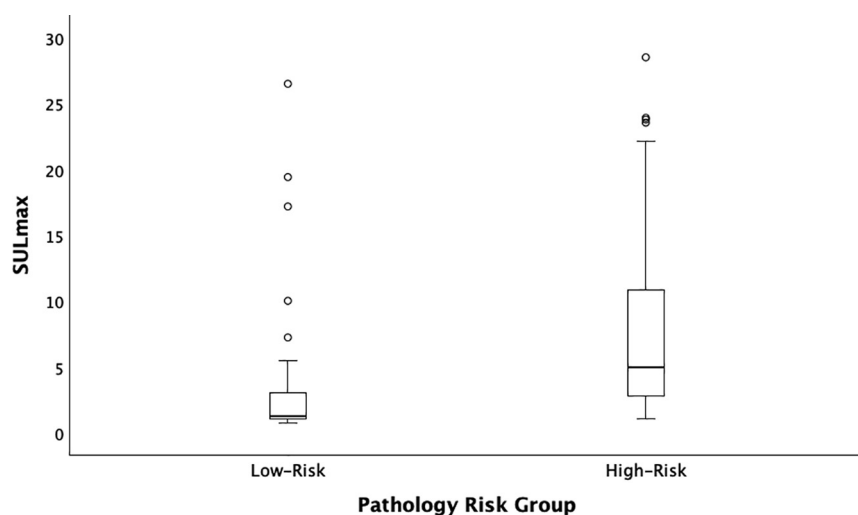


FIG 2. Boxplots illustrating the distribution of SULmax values by pathologic risk. High-risk lesions include anaplastic and PDTC thyroid carcinoma, and low-risk lesions include PTCs and those without residual tumor.

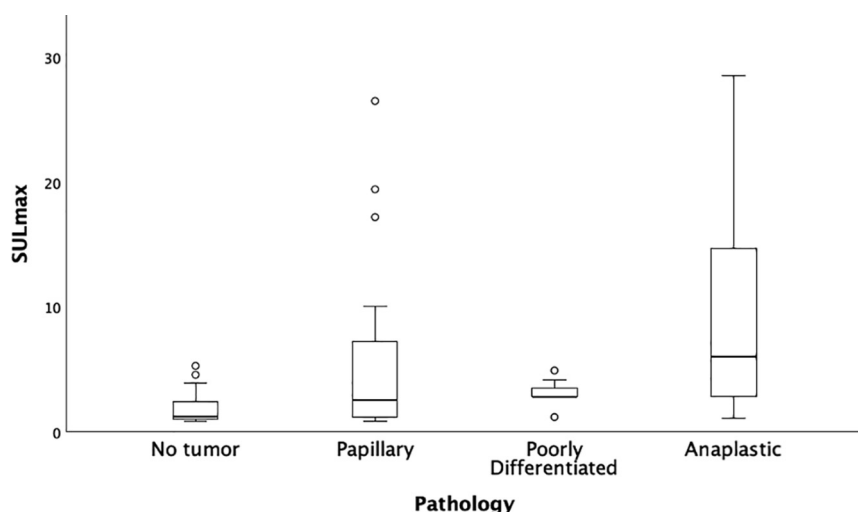


FIG 3. Boxplots illustrating the distribution of SULmax values across all 4 pathologic grades.

The point on the ROC curve with the highest Youden index equal to 0.486 was used to identify the optimal SULmax cutoff for the preoperative identification of high-risk versus low-risk lesions. This threshold was equal to 2.75 and had a sensitivity, specificity, and accuracy of 0.784 [95% CI, 0.628–0.886], 0.702 [95% CI, 0.573–0.805], and 0.734 [95% CI, 0.637–0.813], respectively. In an attempt to provide a more clinically meaningful threshold that would prioritize sensitivity over specificity to rule out high-risk lesions, we identified an SULmax cutoff of 1.36 yielding a sensitivity of 0.919 [95% CI, 0.787–0.972], but with a reduced specificity and accuracy of 0.544 [95% CI, 0.416–0.666] and 0.691 [95% CI, 0.592–0.776], respectively. Contingency tables corresponding to the optimal and clinically meaningful thresholds are available in [Tables 2 and 3](#).

Survival Analysis

At the end of data collection (March 9, 2024), the median postoperative follow-up time was 433 days (IQR 229.3–1403.8). Patients

with at least 1 high-risk lesion on histopathologic examination had a worse prognosis compared with patients without high-risk lesions. The median OS for the former group was 257 days and was not attained for the latter ($P = .004$, logrank test). In fact, 81.8% of patients (9/11) without a high-risk lesion on pathology were alive at the time of follow-up. Similarly, patients with lesions demonstrating an $\text{SULmax} \geq 2.75$ (i.e. the previously identified optimal cutoff to identify high-risk lesions) did worse than those with uptake below this threshold on FDG-PET/CT. The median OS for the former group was 259 days and was not attained for the latter ($P = .038$, log-rank test). Moreover, 75.0% of patients (6/8) without a lesion with $\text{SULmax} \geq 2.75$ survived at the end of follow-up. Kaplan-Meier curves illustrating OS based on pathologic assessment and FDG uptake are illustrated in [Fig 6](#).

DISCUSSION

The results from this study demonstrate the value of FDG-PET in evaluating for sites of residual PDTC and ATC tumors. These histologies were grouped due to their similarly poor long-term survival outcomes relative to PTC, and previous research demonstrating relatively elevated FDG avidity.^{12,19} SULmax values were found to be significantly different between higher-risk (ATC, PDTC) and lower-risk histologies (PTC and negative). For optimal accuracy an SULmax threshold of ≥ 2.75

could identify residual ATC and PDTC with a sensitivity of 78.4% and a specificity of 70.2%, and with an overall accuracy of 73.4% (Youden index 0.49). In the pursuit of maximizing sensitivity an SULmax threshold of ≥ 1.36 could localize residual PDTC and ATC with a sensitivity of 91.9%, but with a degraded specificity of only 54.4%. Notably an SULmax of 1.36 is largely within range of minimally avid physiologic head and neck soft tissue, and thus such a threshold would require essentially any tissue with uptake above background to be regarded with suspicion.

The Kruskal-Wallis post hoc pair-wise comparisons of FDG uptake yielded no significant difference in the median SULmax values when ATC, PDTC, and PTC were individually compared with one another, but with a significant difference noted between ATC and sites negative for all tumor types. ATC is known from prior research to exhibit the highest GLUT1 transporter expression and associated FDG uptake among thyroid neoplasms, making this an overall expected finding.¹² However, this study furthers the understanding of the FDG-PET behavior of ATC by

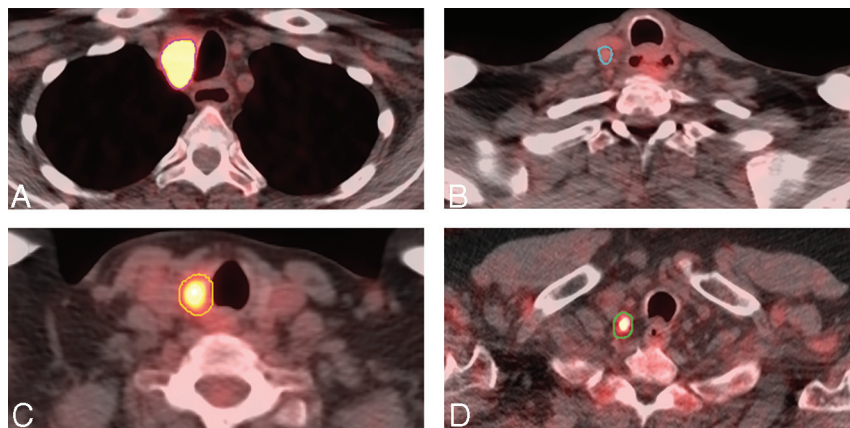


FIG 4. Representative cases for each of the 4 pathologic grades, illustrated with corresponding axial fusion FDG-PET/CT images, uniformly windowed across all studies. A, 66-year-old male patient with ATC stage IVB, status post 1 year of neoadjuvant dabrafenib/trametinib. Preoperative FDG-PET/CT shows a hypermetabolic right paratracheal lesion (purple) with an SULmax = 8.44. Postoperative pathology of this lesion revealed residual ATC. B, Same patient with prominent right level IV lymph node (bright blue) and low FDG uptake (SULmax = 1.58), which is negative for residual tumor on surgical pathology. C, 70-year-old female patient with ATC stage IVB, status post 16 months of neoadjuvant dabrafenib/trametinib. The right thyroid lobe lesion (yellow) on preoperative FDG-PET/CT has an SULmax of 4.92 and harbors PDTC cells on surgical specimen. D, 72-year-old male patient with ATC stage IVC, status post 5 months of neoadjuvant dabrafenib/trametinib. The prominent right level IV lymph node (green) on preoperative FDG-PET/CT has an SULmax of 3.12 and harbors residual PTC cells on biopsy.

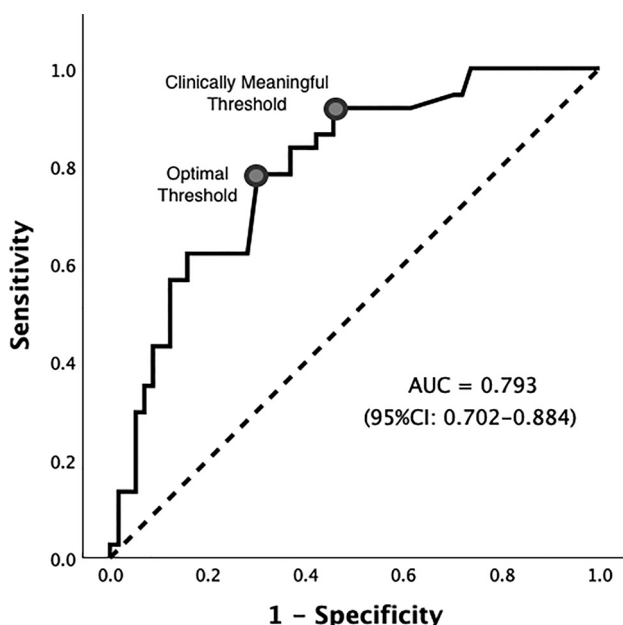


FIG 5. ROC curve for the preoperative classification of lesions as high-risk or low-risk demonstrates an area under the curve of 0.793 [95% CI, 0.702–0.884], indicating acceptable performance of the SULmax-based classifier. An optimal SULmax threshold of 2.75 is identified and can identify high-risk lesions with a sensitivity, specificity, and accuracy of 0.784 [95% CI, 0.628–0.886], 0.702 [95% CI, 0.573–0.805], and 0.734 [95% CI, 0.637–0.813], respectively. A clinically meaningful cutoff of 1.36 is also identified to prioritize a higher sensitivity 0.919 [95% CI, 0.787–0.972] at the expense of the specificity and accuracy (0.544 [95% CI, 0.416–0.666] and 0.691 [95% CI, 0.592–0.776], respectively). Of note, the latter threshold falls within the physiologic range of background soft tissue uptake in the head and neck.

demonstrating its persistent FDG avidity after *BRAF*-directed therapy and emphasizing its potential value in treatment planning after neoadjuvant therapy.

The lack of a significant difference in median SULmax between PTC and negative sites is compatible with previously shown more variable FDG avidity of PTC, ranging from absent to high uptake above background, and which is especially avid in radioactive iodine negative tumors.^{22,23} Moreover, the FDG uptake variability of PTC is qualitatively corroborated by the overlap in SULmax boxplots among ATC, PDTC, and negative sites as seen in Fig 3. The goal of surgical resection after neoadjuvant *BRAF*-directed therapy is largely to resect all sites of residual tumor, regardless of pathologic type. Consequently, while this investigation supports the use of FDG-PET in localizing residual ATC and PDTC, it is unlikely to confidently identify all sites of residual PTC based on our findings.

Accurately localizing the latter will

likely require additional imaging modalities, including dedicated contrast-enhanced neck CT and/or radioactive iodine SPECT/CT.

The degree of FDG uptake at baseline and in follow-up of recurrent thyroid cancer has been shown to be associated with OS, likely largely driven by the underlying histologic type.^{24–27} Given the aforementioned results demonstrating FDG-PET uptake as a useful identifier of residual high-risk pathologies, it was hypothesized that the degree of FDG uptake after *BRAF*-directed therapy could correspondingly demonstrate an association with OS. When patients were dichotomized into those with lesions showing uptake above and below the identified optimal threshold of 2.75 SULmax from the ROC analysis, a statistically significant difference in the survival curves was observed with patients with lesions with SULmax \geq 2.75 showing worse OS. This added prognostic information may prove valuable to oncologists and surgeons as they weigh management options, including proceeding with surgical resection, continuing with another

Table 2: Predicted pathology risk group on FDG-PET/CT by using the optimal SULmax cutoff of 2.75

		Actual Pathology Risk Group		Total
		High-Risk	Low-Risk	
Predicted pathology Risk group	High-risk	29	17	46
	Low-risk	8	40	48
	Total	37	57	94

This cutoff can identify high-risk lesions with a sensitivity, specificity, and accuracy of 0.784 [95% CI, 0.628–0.886], 0.702 [95% CI, 0.573–0.805], and 0.734 [95% CI, 0.637–0.813], respectively.

course of *BRAF*-directed therapy, or pursuing alternative palliative chemotherapy and/or radiation therapy options.

Patients with ATC harboring non-*BRAF* mutations that also have available targeted therapies, such as *ALK* fusions and

ceritinib or *RET* fusions and seliprecatinib, are also recommended to undergo neoadjuvant courses before surgery according to the latest guidelines from the American Thyroid Association.¹¹ A limited number of case reports have looked at nonthyroid solid tumors with these mutations, and found FDG avidity at residual sites of disease following neoadjuvant treatment courses.^{28,29} However, to our knowledge no investigations have addressed this question in the setting of thyroid cancer. Further research will be required to confirm the role of FDG-PET in localizing residual sites of disease in patients with ATC after treatment with these other types of targeted neoadjuvant therapies and in the setting of *BRAF*-wild-type ATC.

This study is in part limited by the predetermined 30-day maximum interval between patient presurgical FDG-PET/CT and their surgical resection date, above which patients were not

included in the study. This criterion was selected so that the underlying pathologic state (eg, residual ATC tumor) at the time of the FDG-PET/CT most closely resembled the pathology results at the time of surgery. Of the 30 patients included in this study, the maximum recorded interval between FDG-PET/CT and surgery was 23 days. It is possible that this window introduced some degree of pathologic discordance, which may have impacted the results of this investigation. The clinical courses of the included patients in this study were also somewhat heterogeneous, including variable rates of surgeries and other chemotherapy regimens preceding *BRAF*-directed therapy, and variable durations of neoadjuvant *BRAF*-directed therapy. These nonuniformities may have exerted uncertain influences on the outcomes of this investigation. Although meticulous review and correlation of FDG-PET/CT findings with operative/pathology reports was performed, in the absence of intraoperative imaging it is not possible to ensure complete concordance between the pathologic specimens and the recorded FDG uptake values. Finally, the small sample size precluded adjustment for potential confounders such as with a multivariate Cox proportional hazards regression analysis.

Table 3: Predicted pathology risk group on FDG-PET/CT by using the clinically meaningful SULmax cutoff of 1.36

		Actual Pathology Risk Group		Total
		High-Risk	Low-Risk	
Predicted pathology	High-risk	34	26	60
Risk group	Low-risk	3	31	34
	Total	37	57	94

Note:—This cutoff can identify high-risk lesions with a sensitivity, specificity, and accuracy of 0.919 [95% CI, 0.787–0.972], 0.544 [95% CI, 0.416–0.666], and 0.691 [95% CI, 0.592–0.776], respectively.

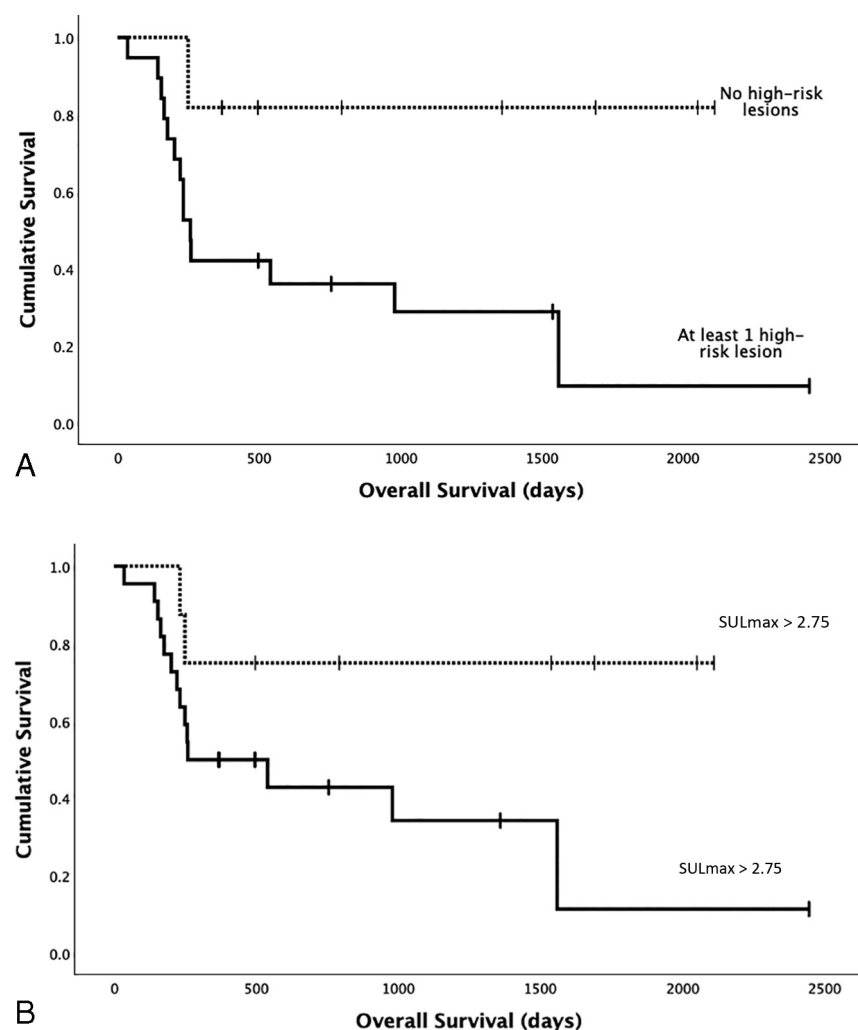


FIG 6. Kaplan-Meier curves comparing OS in patients with at least 1 high-risk lesion versus no high-risk lesion in the head and neck based on pathology results and FDG uptake. A, When pathologic risk group is determined via histopathologic assessment of surgically sampled specimens, median OS is 257 days for patients with at least 1 high-risk lesion versus not attained in patients with no high-risk lesions ($P = .004$, log-rank test). The right-censored cumulative survival for the latter group at the end of follow-up was 81.8% (9/11). B, When SULmax of 2.75 is used as a proxy for high-risk lesions, median OS is 259 days for patients with at least 1 lesion with $\text{SULmax} \geq 2.75$ versus not attained in patients without lesion with $\text{SULmax} \geq 2.75$ ($P = .038$, log-rank test). The right-censored cumulative survival for the latter group at the end of follow-up was 75.0% (6/8).

CONCLUSIONS

This study evaluates the performance of FDG-PET/CT in assessing for residual high-risk histologic subtypes ATC and PDTC after *BRAF*-directed therapy and immunotherapy. Clinicians can use the degree of FDG uptake, in

conjunction with other factors, to assess the probability that an anatomic site harbors residual tumor, but with the recognition that sites of lower-grade tumor (ie, PTC) may be missed. Despite the latter constraint, FDG-PET/CT can still serve as an effective clinical tool to guide patient management, including planning the extent of surgical resections and predicting prognosis.

Disclosure forms provided by the authors are available with the full text and PDF of this article at www.ajnr.org.

REFERENCES

- Hundahl SA, Fleming ID, Fremgen AM, et al. **A National Cancer Data Base report on 53,856 cases of thyroid carcinoma treated in the U.S., 1985-1995** [see comments]. *Cancer* 1998;83:2638-48 [CrossRef](#)
- Xu B, Fuchs T, Dogan S, et al. **Dissecting anaplastic thyroid carcinoma: a comprehensive clinical, histologic, immunophenotypic, and molecular study of 360 cases**. *Thyroid* 2020;30:1505-17 [CrossRef](#) [Medline](#)
- Zhang K, Wang X, Wei T, et al. **Comparative study between poorly differentiated thyroid cancer and anaplastic thyroid cancer: real-world pathological distribution, death attribution, and prognostic factor estimation**. *Front Endocrinol (Lausanne)* 2024;15:1347362 [CrossRef](#) [Medline](#)
- Wang JR, Montierth M, Xu L, et al. **Impact of somatic mutations on survival outcomes in patients with anaplastic thyroid carcinoma**. *JCO Precis Oncol* 2022;6:e2100504 [CrossRef](#) [Medline](#)
- DailyMed. **TAFINLAR-dabrafenib capsule TAFINLAR-dabrafenib tablet, for suspension**. <https://dailymed.nlm.nih.gov/dailymed/drugInfo.cfm?setid=fe1e6b1-e1a5-4254-9f2e-a70e0f8dbdea>
- Hamidi S, Dadu R, Zafereo ME, et al. **Initial management of BRAF V600E-variant anaplastic thyroid cancer: the FAST Multidisciplinary Group Consensus Statement**. *JAMA Oncol* 2024;10:1264-71 [CrossRef](#) [Medline](#)
- Maniakas A, Dadu R, Busaidy NL, et al. **Evaluation of overall survival in patients with anaplastic thyroid carcinoma, 2000-2019**. *JAMA Oncol* 2020;6:1397-404 [CrossRef](#)
- Zhao X, Wang JR, Dadu R, et al. **Surgery after BRAF-directed therapy is associated with improved survival in BRAFV600E mutant anaplastic thyroid cancer: a single-center retrospective cohort study**. *Thyroid* 2023;33:484-91 [CrossRef](#)
- Hamidi S, Iyer PC, Dadu R, et al. **Checkpoint inhibition in addition to dabrafenib/trametinib for BRAFV600E-mutated anaplastic thyroid carcinoma**. *Thyroid* 2024;34:336-46 [CrossRef](#) [Medline](#)
- National Comprehensive Cancer Network. **NCCN Clinical Practice Guidelines in Oncology Thyroid Carcinoma** 2024:54-59. <https://www.nccn.org/guidelines/guidelines-detail?category=1&id=1470>
- Bible KC, Kebebew E, Brierley J, et al. **2021 American Thyroid Association Guidelines for Management of Patients with Anaplastic Thyroid Cancer**. *Thyroid* 2021;31:337-86 [CrossRef](#)
- Grabellus F, Nagarajah J, Bockisch A, et al. **Glucose transporter 1 expression, tumor proliferation, and iodine/glucose uptake in thyroid cancer with emphasis on poorly differentiated thyroid carcinoma**. *Clin Nucl Med* 2012;37:121-27 [CrossRef](#)
- Bossuyt PM, Reitsma JB, Bruns DE, et al; STARD Group. **STARD 2015: an updated list of essential items for reporting diagnostic accuracy studies**. *Radiology* 2015;277:826-32 [CrossRef](#)
- Robbins KT, Shaha AR, Medina JE, et al; Committee for Neck Dissection Classification, American Head and Neck Society. **Consensus Statement on the Classification and Terminology of Neck Dissection**. *Arch Otolaryngol Head Neck Surg* 2008;134:536-38 [CrossRef](#) [Medline](#)
- Sugawara Y, Zasadny KR, Neuhoff AW, et al. **Reevaluation of the standardized uptake value for FDG: variations with body weight and methods for correction**. *Radiology* 1999;213:521-25 [CrossRef](#) [Medline](#)
- Zasadny KR, Wahl RL. **Standardized uptake values of normal tissues at PET with 2-[fluorine-18]-fluoro-2-deoxy-D-glucose: variations with body weight and a method for correction**. *Radiology* 1993;189:847-50 [CrossRef](#)
- Wahl RL, Jacene H, Kasamon Y, et al. **From RECIST to PERCIST: evolving considerations for PET response criteria in solid tumors**. *J Nucl Med* 2009;50:122S-50S [CrossRef](#)
- Ibrahimipasic T, Ghossein R, Shah JP, et al. **Poorly differentiated carcinoma of the thyroid gland: current status and future prospects**. *Thyroid* 2019;29:311-21 [CrossRef](#)
- Nagarajah J, Ho AL, Tuttle RM, et al. **Correlation of BRAFV600E mutation and glucose metabolism in thyroid cancer patients: an 18F-FDG PET study**. *J Nucl Med* 2015;56:662-67 [CrossRef](#)
- Youden WJ. **Index for rating diagnostic tests**. *Cancer* 1950;3:32-35 [CrossRef](#)
- Ruopp MD, Perkins NJ, Whitcomb BW, et al. **Youden index and optimal cut-point estimated from observations affected by a lower limit of detection**. *Biometrical J* 2008;50:419-30 [CrossRef](#)
- Grünwald F, Källicke T, Feine U, et al. **Fluorine-18 fluorodeoxyglucose positron emission tomography in thyroid cancer: results of a multicentre study**. *Eur J Nucl Med* 1999;26:1547-52 [CrossRef](#) [Medline](#)
- Kim H, Na KJ, Choi JH, et al. **Feasibility of FDG-PET/CT for the initial diagnosis of papillary thyroid cancer**. *Eur Arch Otorhinolaryngol* 2016;273:1569-76 [CrossRef](#) [Medline](#)
- Kim HJ, Chang H-S, Ryu YH. **Prognostic role of pre-treatment [18F]FDG PET/CT in patients with anaplastic thyroid cancer**. *Cancers (Basel)* 2021;13:4228 [CrossRef](#)
- Pryma DA, Schöder H, Gönen M, et al. **Diagnostic accuracy and prognostic value of 18F-FDG PET in Hürthle cell thyroid cancer patients**. *J Nucl Med* 2006;47:1260-66 [Medline](#)
- Schreinemakers JM, Vriens MR, Munoz-Perez N, et al. **Fluorodeoxyglucose-positron emission tomography scan-positive recurrent papillary thyroid cancer and the prognosis and implications for surgical management**. *World J Surg Oncol* 2012;10:192 [CrossRef](#) [Medline](#)
- Manohar P, Beesley LJ, Bellile E, et al. **Prognostic value of FDG-PET/CT metabolic parameters in metastatic radioiodine refractory differentiated thyroid cancer**. *Clin Nucl Med* 2018;43:641-47 [CrossRef](#) [Medline](#)
- Mansfield AS, Murphy SJ, Harris FR, et al. **Chromoplectic TPM3-ALK rearrangement in a patient with inflammatory myofibroblastic tumor who responded to ceritinib after progression on crizotinib**. *Ann Oncol* 2016;27:2111-17 [CrossRef](#) [Medline](#)
- Schrenk KG, Weschenfelder W, Spiegel C, et al. **Exceptional response to neoadjuvant targeted therapy with the selective RET inhibitor selpercatinib in RET-fusion-associated sarcoma**. *J Cancer Res Clin Oncol* 2023;149:5493-96 [CrossRef](#) [Medline](#)
- Tuttle RM, Haugen B, Perrier ND. **Updated American Joint Committee on Cancer/Tumor-Node-Metastasis Staging System for Differentiated and Anaplastic Thyroid Cancer (Eighth Edition): What Changed and Why?** *Thyroid* 2017;27:751-56 [CrossRef](#) [Medline](#)